
Interactive
comment

Interactive comment on “Formation and origin of Fe-Si oxyhydroxide deposits at the ultra-slow spreading Southwest Indian Ridge” by Kaiwen Ta et al.

Kaiwen Ta et al.

takaiwen@sidsse.ac.cn

Received and published: 3 March 2020

Response to Reviewer

All of us would like to thank the editor and reviewer again for your considerations about this manuscript and constructive comments. We have revised it very carefully. Responses are provided in a point-by-point fashion.

Interactive comment on “Formation and origin of Fe-Si oxyhydroxide deposits at the ultra-slow spreading Southwest Indian Ridge” by Kaiwen Ta et al. Anonymous Referee #1 Received and published: 17 January 2020

[Printer-friendly version](#)

[Discussion paper](#)



Interactive
comment

RC1: The manuscript by Kaiwen Ta et al. presents a rather exhaustive panoply of analytical techniques performed on samples from six exhalative Fe-Si deposits collected during a cruise in the SW Indian Ridge. The authors conclude that their analysis show that these deposits are of low temperature, mainly made of Fe-Si and that there is a strong biological influence in their formation. They also present Sr-Nd-Pb isotope that seem to support their conclusions. The topic can be of major interest for the readers of Biogeosciences. However, my opinion is that the manuscript needs major and complete rewriting before being considered for publication – is too repetitive, phrases are vague and is not clearly shown what these techniques really add to the state of the art. Writing is extremely repetitive and the text should be checked by an English-speaking specialist.

Answer: Thanks for the reviewer's constructive comments. In the revised version, we have rewritten the manuscript to enhance readability based on your suggestion. We have made considerable efforts to improve the grammar of manuscript.

RC1: Also, I have the feeling that the authors have used different exciting and novel techniques but without having a clear focus in what they try to show. I would suggest to careful evaluate if the use of these techniques adds something to the interpretation of these rocks that could well easily done with some basic geology and a conventional petrographic-chemical analysis.

Answer: Thanks for the reviewer's constructive comments. We have added more discussions on some basic geology and a conventional petrographic-chemical analysis to the interpretation of these rocks in the revised paper.

RC1: Finally, I have serious doubts that the authors are able to prove that these structures found in the iron oxydehydroxyde deposits and silica precipitates represent fossilized microbes despite your are within the life thermal window. By aware that inorganic silica growth, just an example, can mask organic textures (see, for example, Garcia Ruiz et al 2017, Science). For being sure that these structures represent past

[Printer-friendly version](#)

[Discussion paper](#)



Interactive comment

organic activity you must show TEM images and/or some stable isotopes indicative of biogenic-promoted redox equilibria. If in active sites, you should try some geomicrobiological studies.

Answer: Thanks for providing valuable information on the biogenic structures distinguishing from inorganic silica growth. We have added TEM images and EDS date to discuss these Fe oxyhydroxide stalks potentially represented past organic activity (Fig. S3). We have also tried some geomicrobiological studies to culture Fe-oxidizing bacteria according to the reviewer's suggestion. We observed that Fe-stalks were produced by Fe-oxidizing bacteria similar to morphologies of Fe-Si oxyhydroxides in studied deposits (Fig. S4). We suggested that these structures found in the iron oxydehydroxyde deposits and silica precipitates represented the microbes encrusted by Fe-Si oxydehydroxydes.

RC1: Finally, all the radiogenic isotope geochemistry needs some reinterpretation. Pb isotopes are not just indicative of major hydrothermal activity -that is saying nothing in terms of radiogenic isotope geochemistry.

Answer: Thanks for this valuable comment. We have rewritten the manuscript on all the radiogenic isotope geochemistry in the revised paper.

RC1: The statement that Sr-Nd isotopes “were closely related to interaction between hydrothermal fluids and seawater” is also ambiguous.

Answer: Thanks for your consideration. We have revised them in the manuscript as following: Sr and Nd isotope compositions of Fe-Si oxyhydroxide deposits at the SWIR probably reflected a combined signature of the hydrothermal fluid and seawater.

RC1: Obviously, there must a significant part of the Sr inherited from seawater but the hydrothermal fluids must transport some also.

Answer: We agree with the reviewer that there is a significant part of the Sr in the Fe-Si oxyhydroxide deposits at the SWIR inherited from seawater, but the hydrothermal fluids

[Printer-friendly version](#)

[Discussion paper](#)



must also transport some.

RC1: Nd is unlikely to be derived from seawater and perhaps the Nd isotope signature should be controlled by the hydrothermal fluid – mixing diagrams are fundamental for this discussion. But a key unresolved question is where the deep fluids come from? Probably they are equilibrated with oceanic crust but this needs to be discussed.

Answer: Thanks for the reviewer's constructive comments. We have added hydrothermal fluid – mixing diagrams to discuss on Nd isotope signature (Fig. 8). We have also added more discussions that the deep fluids probably acted to equilibrate the hydrothermal fluid with oceanic crust, according to the reviewer's suggestions in the revised paper.

RC1: Please check ambiguous phrases such as “appropriate solvent” or be aware of the analytical error when quoting stable isotopes – you cannot go to the second decimal.

Answer: Thank you for pointing them out. We have corrected them in the revised paper as following: The different solvents would subsequently extract the following phases: 1 M Na-acetate, 1 M hydroxylamine-HCl, 0.28 M Na-dithionite and 12 M HCl, for a defined period of time (Table S2).

RC1: Also, you cannot go to the second!! decimal when calculating isotope temperatures. Errors here are usually above $\pm 20 \text{ }^\circ\text{C}$. You have to explain how this was calculated. The same holds true for Pb isotopes... 4th decimal!! Please, have all these data checked by an specialist in isotope geochemistry.

Answer: Sorry for these mistakes. We have corrected them in the revised paper (Table 2).

RC1: You say that positive eNd values are indicative of a mantle derivation – that is ok but you can say a lot more with your data. And what about the negative values? Your reservoir looks really heterogeneous and this ample range of eNd values need to be

[Printer-friendly version](#)

[Discussion paper](#)



Interactive
comment

discussed.

Answer: Thanks for this valuable comment. We have added more discussions on this ample range of eNd values in the revised paper as following:

The mixing between hydrothermal fluids and seawater was likely reflected by Nd isotopic data of the deposits. In order to better understand the mixing relationship between hydrothermal fluids and seawater, ΔNd versus $^{87}\text{Sr}/^{86}\text{Sr}$ correlation for Fe-Si oxyhydroxide deposits was compared to hydrothermal fluid and seawater in Figure 8. The Nd-Sr isotope mixing model indicated that samples 20V-T8 and 34II-T22 had higher ΔNd values (3.2 and 5.1) than modern Indian Ocean seawater values (-8.0) (Pomiès et al., 2002) and were close to the values of hydrothermal fluid (7.1) (Amini et al., 2008). We inferred that Nd in two samples was mainly derived from hydrothermal fluid, which was produced by seawater leaching basalt at elevated temperatures (Fig. 8). The presence of a positive Eu anomaly in the Fe-Si oxyhydroxide deposits further supported this interpretation. On the other hand, negative ΔNd values indicated incorporation of abundant seawater Nd into the Fe-Si oxyhydroxide deposits. This result may attribute to an extremely low extent of seawater-basalt interaction during the hydrothermal circulation. Alternatively, negative ΔNd values of DIV95-1, DIV95-2, 21V-T1 and 21V-T7 samples possibly reflected the interaction between Fe-Si oxyhydroxides and seawater (Clauer et al., 1984). Baker et al. (1987) suggested hydrothermal circulation may play a significant role in the geochemical composition of the oceanic crust and seawater (Baker et al., 1987). Coupled fluid flow and chemical exchange probably acted to equilibrate the hydrothermal fluid with oceanic crust and modulate the chemistry of the hydrothermal field (Mottl, 2003). We proposed that the Sr and Nd isotope compositions of the Fe-Si oxyhydroxide deposits at the SWIR might be closely related to mixing between hydrothermal fluids and seawater.

RC1: The same for Sr isotopes. Your range of data is extremely variable, is not a “slight variation” going from 0.7079 to 0.7091 and you need to explain this – not done in the manuscript.

[Printer-friendly version](#)

[Discussion paper](#)



Answer: Thanks for the reviewer's constructive comments. We have moderated them in the revised paper as following:

The Sr isotopic compositions of the deposits were extremely variable ($^{87}\text{Sr}/^{86}\text{Sr} = 0.70794\text{--}0.70915$), and had values indistinguishable from present-day seawater ($^{87}\text{Sr}/^{86}\text{Sr} = 0.70918$) (Peucker-Ehrenbrink and Fiske, 2019).

RC1: Also, you are talking about oxidized systems and you quote pyrite by XRD. How abundant is the pyrite? Where it is located? Is it the primary mineral that has been extensively oxidized? Or pyrite is just a local precipitate in a more anoxic setting? The low S contents today do not prove that these rocks were originally precipitated as sulphide rocks and later being oxidized. You must have stronger arguments. These questions need to be solved by just careful observations before performing a batch of uncontrolled analytical techniques. Also, you must try to interpret all your results, even if contradictory, not just some of them.

Answer: Sorry for this mistake about the pyrite by XRD, and so at this point we have carefully reanalyzed XRD data. We think that pyrite is not determined in the hydrothermal Fe-Si oxyhydroxide deposits by XRD. We appreciate reviewer for reminding us on the discussion. We have revised the manuscript to be more clear about the XRD results as following:

The XRD results showed that 2-line ferrihydrite, hematite, nontronite, opal and birnessite composed the major minerals in the samples (Fig. S2). In the spectra of samples 21V-T7, 21V-T1 and 20V-T8, a broad peak centered at 4.08 \AA suggested the presence of opal. The spectral peaks appeared at 2.69 \AA and 1.60 \AA in samples DIV95-1, DIV95-2, 21V-T7, 21V-T1 and 20V-T8 indicated the presence of hematite. The spectral signature of birnessite was most clearly observed in sample DIV95-2, at $d = 7.06$ and 2.45 \AA . A small amount of birnessite was observed in DIV95-1, which was presumed to be from the residual black layer. Poorly crystalline two-line ferrihydrite, characterized by the appearance of peaks at $d = 2.62 \text{ \AA}$ and 1.51 \AA , was the principal mineral ob-

[Printer-friendly version](#)

[Discussion paper](#)



Interactive comment

served in the spectra of samples DIV95-2 and 34II-T22. Nontronite was also present in 34II-T22 deposit. In addition, halite was observed in our samples, which presumably was formed by evaporation.

RC1: Unless you unambiguously prove direct or indirectly, that the structures are microbial the major conclusions of the paper should be considered just an attractive but plausible hypothesis.

Answer: Thanks for the reviewer's constructive comments. We have added TEM images and EDS date to support the structures belong to microbial formation. Furthermore, we have also tried to culture Fe-oxidizing bacteria from these Fe-Si oxyhydroxides. We observe that Fe-stalks are produced by Fe-oxidizing bacteria similar to morphologies of Fe-Si-oxyhydroxides in studied deposits (Fig. S4). We suggest that these structures found in the iron oxydehydroxyde deposits and silica precipitates represent the microbes encrusted by Fe-Si oxydehydroxydes.

RC1: Don't go too far into speculative conclusions before being sure of that. The discussion needs to be completely rewritten but probably the aforementioned aspects need to be solved before getting into a thoughtful review.

Answer: We have deleted some too far into speculative conclusions, for example: "biogenic Fe-Si oxyhydroxides probably tie in the origin and evolution of life" in the revised paper. We have rewritten the discussion and conclusion to enhance readability based on the reviewer's suggestions in the revised paper.

Please also note the supplement to this comment:

<https://www.biogeosciences-discuss.net/bg-2019-315/bg-2019-315-AC1-supplement.pdf>

Interactive comment on Biogeosciences Discuss., <https://doi.org/10.5194/bg-2019-315>, 2019.

Printer-friendly version

Discussion paper



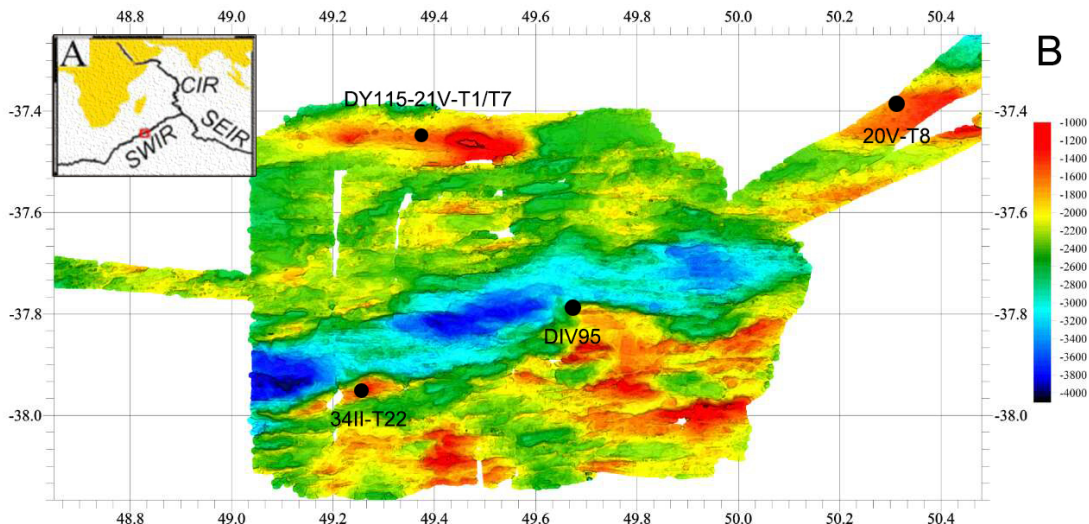


Fig. 1. Regional bathymetric map and location of the sampling site at the SWIR. Black dots represent sample locations in this study.

[Printer-friendly version](#)

[Discussion paper](#)



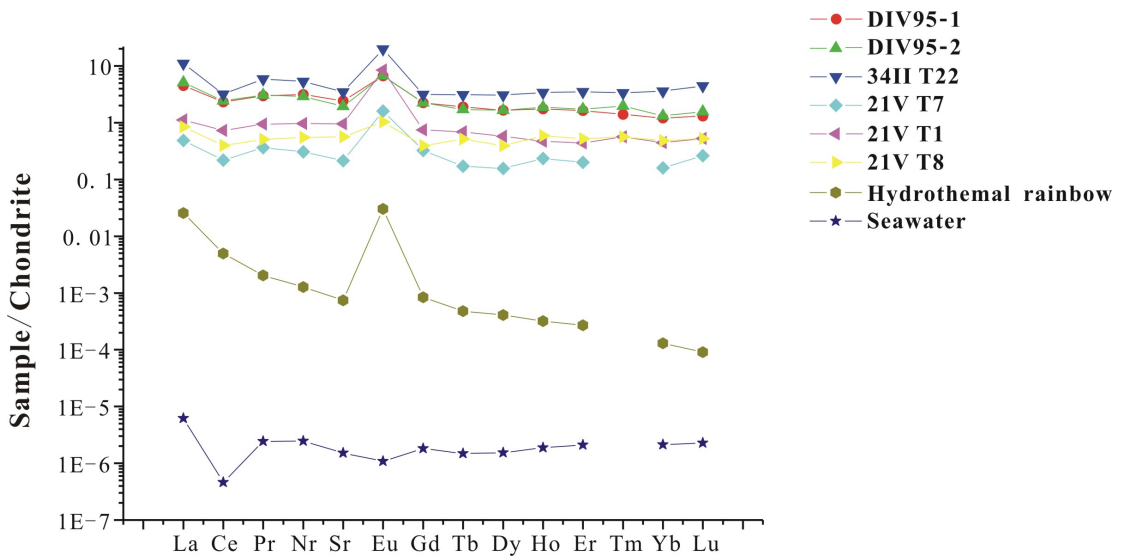


Fig. 2. Chondrite-normalized REE distribution patterns of the hydrothermal Fe-Si oxyhydroxide deposits in this study.

[Printer-friendly version](#)

[Discussion paper](#)



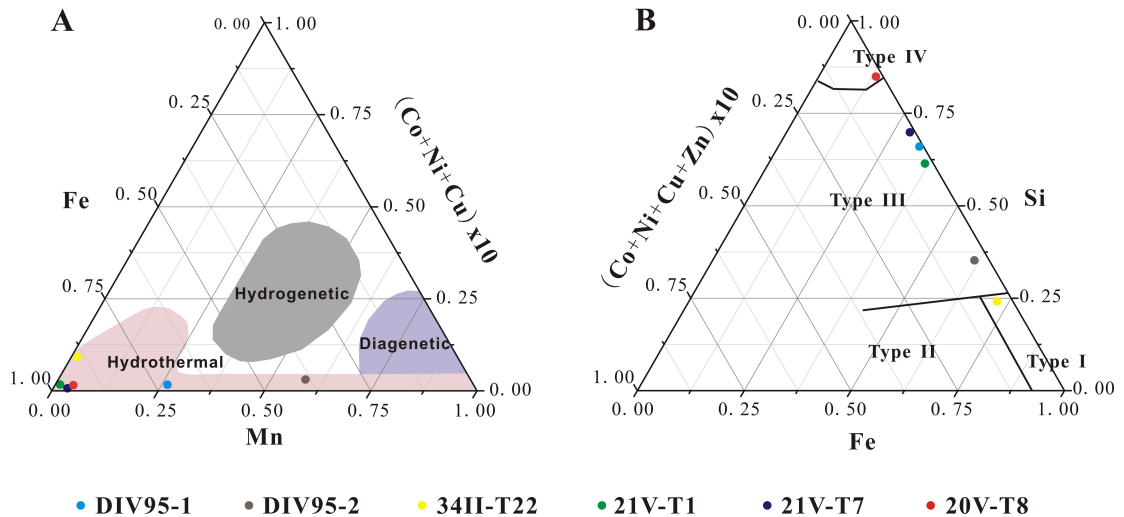


Fig. 3. (a) Ternary diagram for Mn-Fe-(Co + Ni + Cu) $\times 10$ of Fe-Si oxyhydroxide deposits. The hydrothermal, diagenetic and hydrogenous fields were classified by Hein et al. (1994). The Fe-Si oxyhydroxide depos

[Printer-friendly version](#)

[Discussion paper](#)



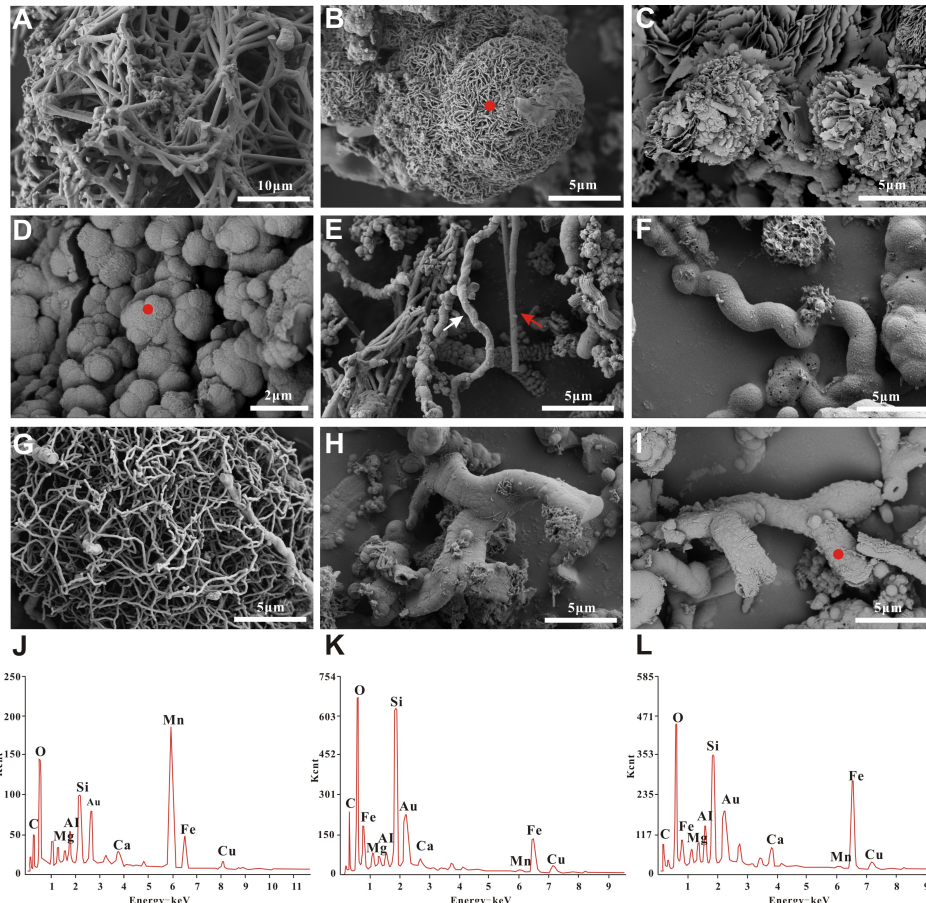


Fig. 4. SEM images showing different styles of biogenic mineral structures in different Fe-Si oxyhydroxide deposits. (a) A network-like structure composed of rod-like mineralized forms observed in the orange-

[Printer-friendly version](#)

[Discussion paper](#)



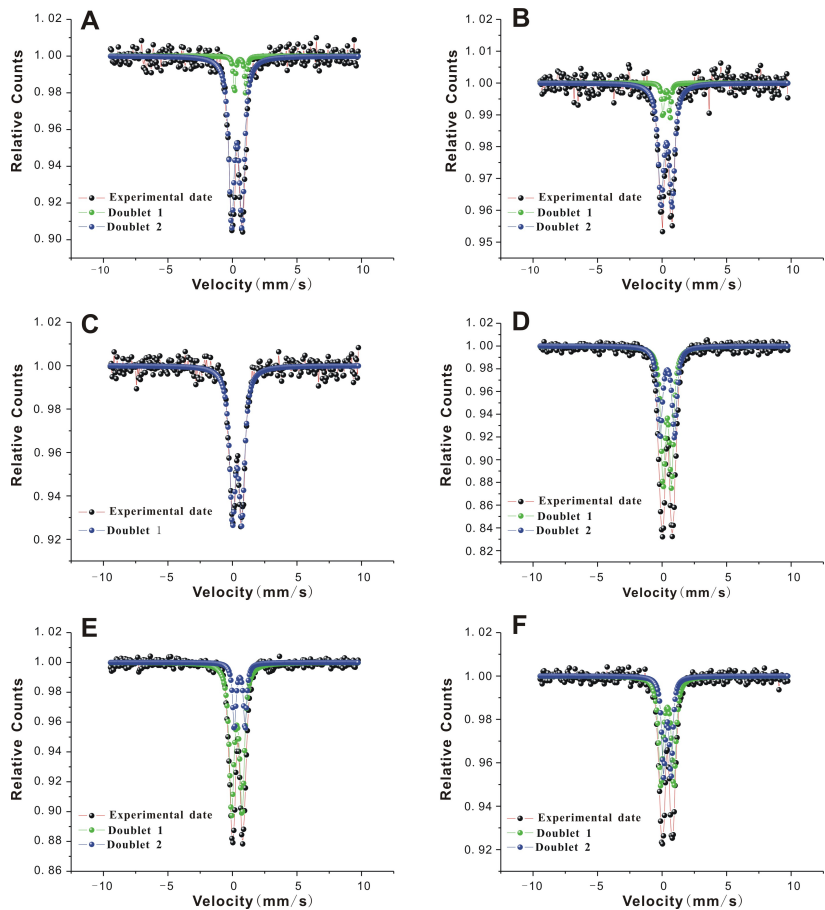


Fig. 5. 57Fe Mössbauer spectra at room temperature (300 K), and fitting results of Fe-Si oxyhydroxide deposits from the SWIR. (a) DIV95-1, (b) DIV95-2, (c) 34II-T22, (d) 21V-T1, (e) 21V-T7, (f) 20V-T8.

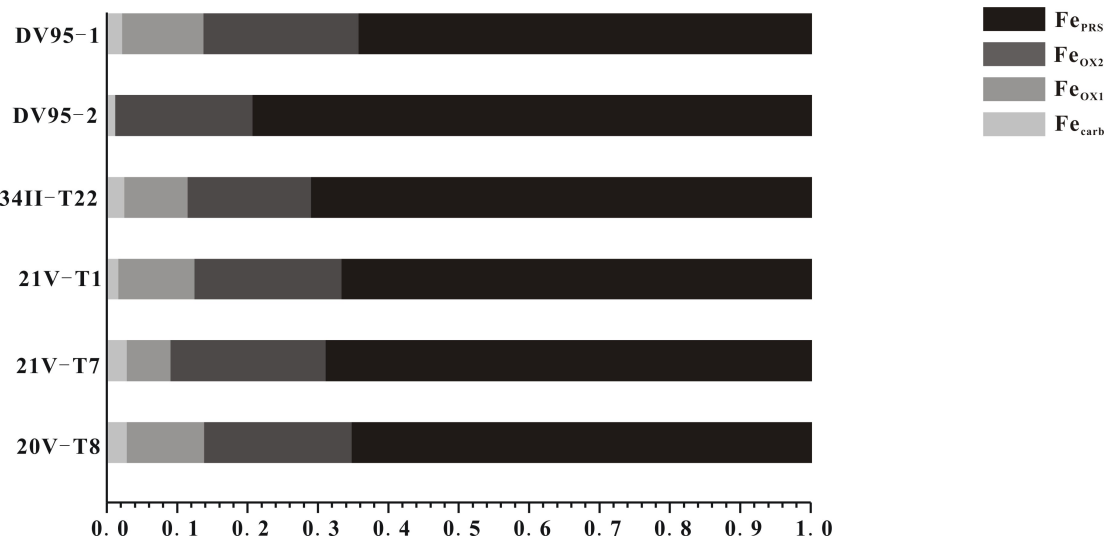


Fig. 6. Sequential extraction of iron minerals in the studied Fe-Si oxyhydroxide deposits.

[Printer-friendly version](#)

[Discussion paper](#)



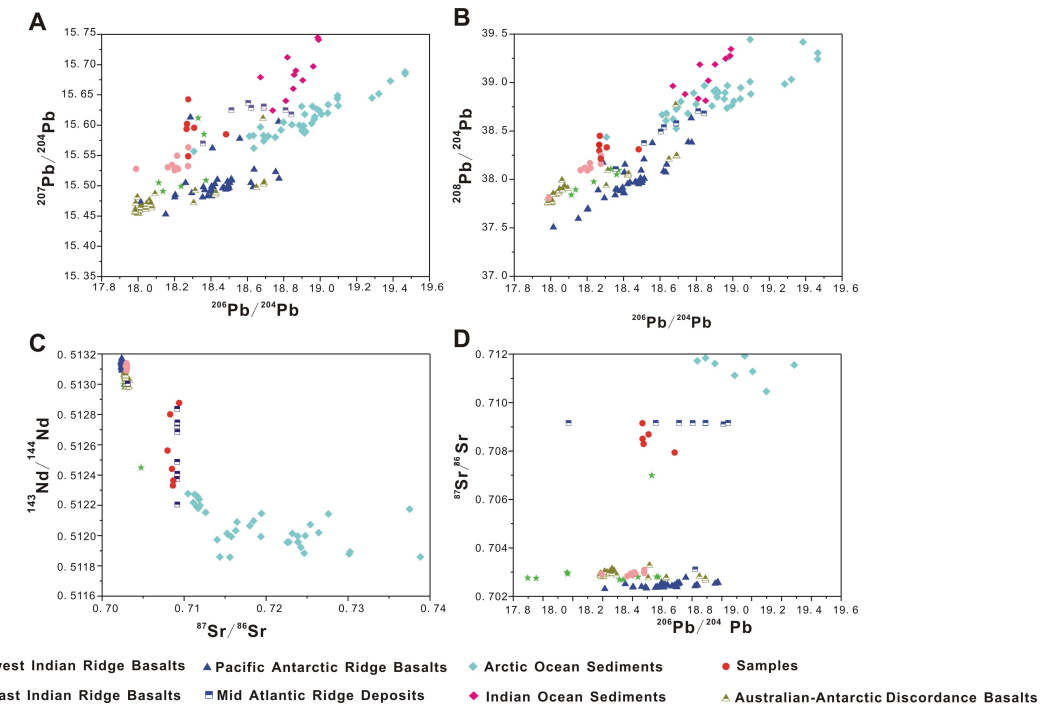
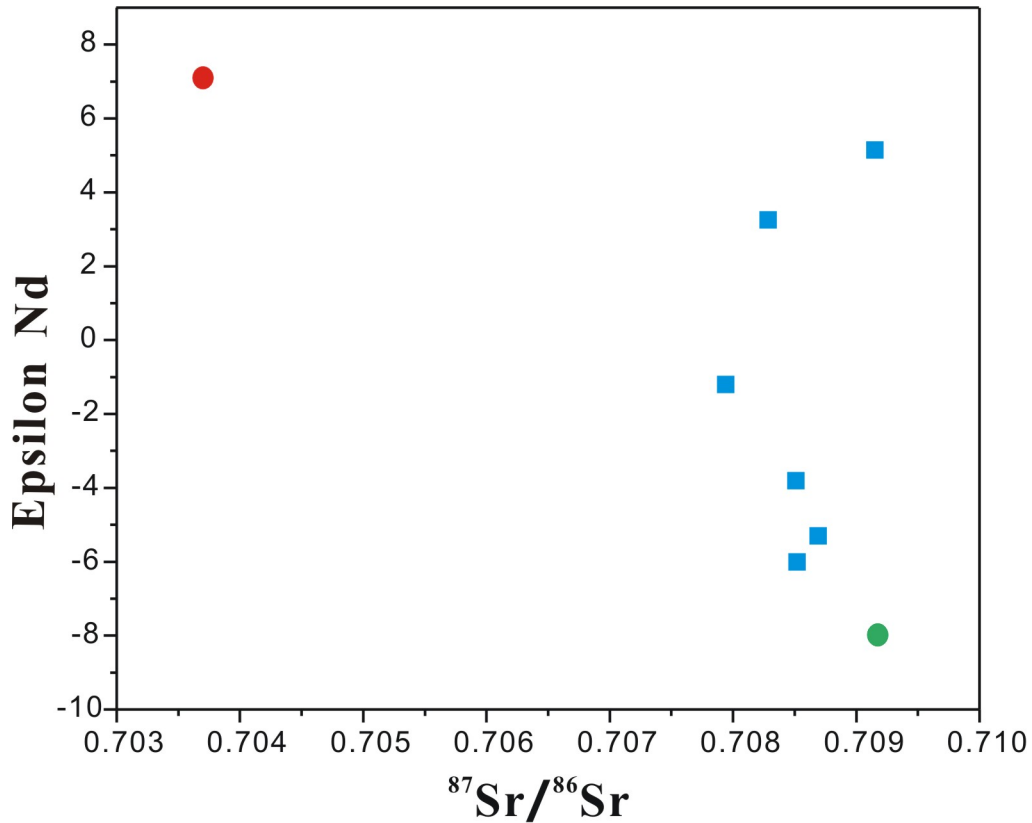


Fig. 7. Comparison of $^{208}\text{Pb}/^{204}\text{Pb}$ versus $^{206}\text{Pb}/^{204}\text{Pb}$ (a), $^{207}\text{Pb}/^{204}\text{Pb}$ versus $^{206}\text{Pb}/^{204}\text{Pb}$ (b), $^{87}\text{Sr}/^{86}\text{Sr}$ versus $^{143}\text{Nd}/^{144}\text{Nd}$ (c), and $^{87}\text{Sr}/^{86}\text{Sr}$ versus $^{206}\text{Pb}/^{204}\text{Pb}$ from the studied deposits, compared against Pac

[Printer-friendly version](#)

[Discussion paper](#)





● Hydrothermal fluids

● Seawater

■ Samples

Fig. 8. Epsilon Nd versus $^{87}\text{Sr}/^{86}\text{Sr}$ for Fe-Si oxyhydroxides compared to hydrothermal fluid and seawater. Isotopic compositions of Nd and Sr based on modern Indian Ocean seawater values ($\epsilon_{\text{Nd}} = -8.0$, $^{87}\text{Sr}/^{86}\text{Sr}$

BGD

Interactive comment

Printer-friendly version

Discussion paper



Interactive
comment

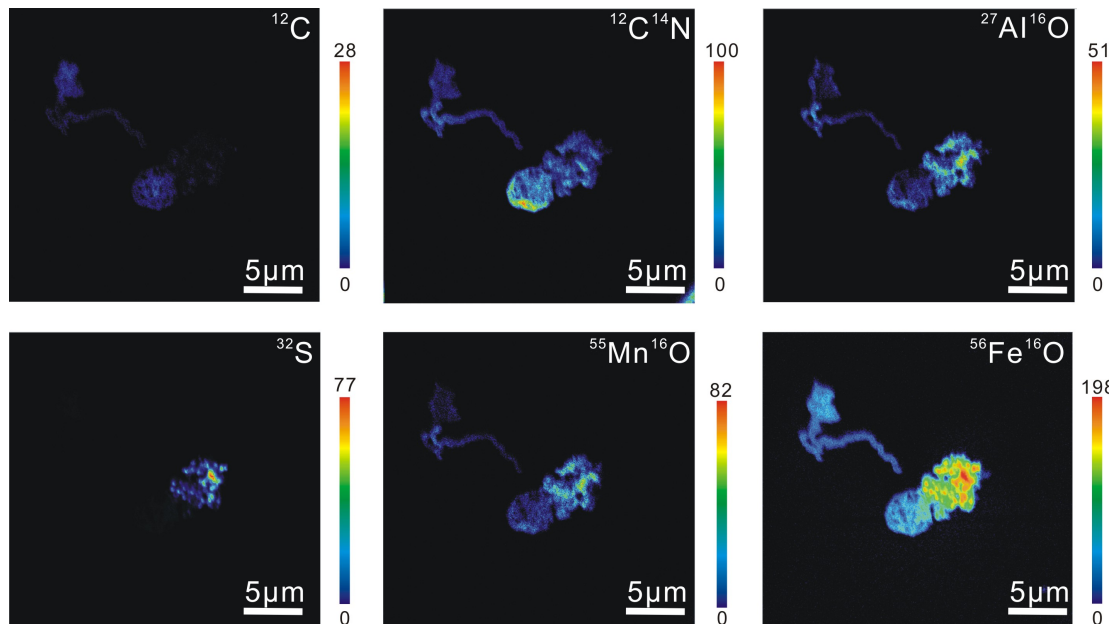


Fig. 9. NanoSIMS ionic images of $^{12}\text{C}-$, $^{12}\text{C}^{14}\text{N}-$, $^{32}\text{S}-$, $^{27}\text{Al}^{16}\text{O}-$, $^{55}\text{Mn}^{16}\text{O}-$, and $^{56}\text{Fe}^{16}\text{O}_2-$ from a twisted stalk. Ion intensity variations were shown by calibration bars. The scale bar was 5 μm for each panel.

[Printer-friendly version](#)

[Discussion paper](#)



Interactive
comment

Table 2. Pb, Sr, Nd, and O isotopic data for studied samples and deduced temperature.

Sample ^a	$^{87}\text{Sr}/^{86}\text{Sr}$	(2 σ)	$^{143}\text{Nd}/^{144}\text{Nd}$	(2 σ)	$^{206}\text{Pb}/^{204}\text{Pb}$	(2 σ)	$^{207}\text{Pb}/^{204}\text{Pb}$	(2 σ)	$^{208}\text{Pb}/^{204}\text{Pb}$	(2 σ)	$^{147}\text{Sm}/^{144}\text{Nd}$	ϵNd	$\delta^{18}\text{O}$ (% SMOW)	Deduced temperature (°C)
DIV95-1	0.70851	0.000014	0.512441	0.000011	18.267	0.003	15.601	0.003	38.296	0.012	0.1416	-3.8	20.9	43.2
DIV95-2	0.70869	0.000013	0.512364	0.000011	18.307	0.003	15.595	0.003	38.331	0.009	0.1298	-5.3	/	/
34II-T22	0.70915	0.000012	0.512895	0.000015	18.266	0.002	15.594	0.002	38.357	0.006	0.1180	5.1	35.8	114.2
21V-T1	0.70852	0.000015	0.512332	0.000015	18.269	0.002	15.640	0.003	38.449	0.006	0.1645	-6	17.3	31.0
21V-T7	0.70794	0.000013	0.512578	0.000031	18.483	0.003	15.585	0.003	38.310	0.009	0.1924	-1.2	16.5	28.6
20V-T8	0.70830	0.000012	0.512801	0.000015	18.275	0.001	15.549	0.001	38.214	0.003	0.1721	3.2	20.5	41.8

Printer-friendly version

Discussion paper

**Fig. 10.**